Desalination and Water Treatment
www.deswater.com

doi: 10.5004/dwt.2018.21866

109 (2018) 145–151
March

Magnetic FeO_x-NdFeB@AC catalyst application in degradation of coking wastewater by activated persulfate process

Chunwei Yang[a,b], Baixiang Ren[a,b,*], Dong Wang[c]

[a]*Key Laboratory of Environmental Materials and Pollution Control, Jilin Normal University, Siping, China, Tel. +86 13694001403; email: m13351582526@163.com (B. Ren), Tel. 13694001402; email: chunwei_yang@jlnu.edu.cn (C. Yang)*
[b]*College of Environmental Science and Engineering, Jilin Normal University, Siping, China*
[c]*School of Environmental Science and Technology, Dalian University of Technology, Dalian, China, Tel. 13940950507; email: wangdong@dlut.edu.cn*

Received 4 August 2017; Accepted 31 December 2017

ABSTRACT

Magnetic NdFeB loading on an activated carbon catalyst (FeO_x-NdFeB@AC) was achieved by a negative pressure impregnation method in this study. The results of magnetic performance tests show that the FeO_x-NdFeB@AC has hard magnetic properties. The surface morphology and composition test results indicated that the specific area and Fe content of FeO_x-NdFeB@AC were significantly improved by the negative pressure impregnation treatment. The feasibility of the FeO_x-NdFeB@AC as a catalyst in an activated persulfate process was studied by degrading real coking wastewater. The results showed that the FeO_x-NdFeB@AC had splendid catalytic activity. Under optimum conditions (pH 3.0, temperature = 40°C, concentration of FeO_x-NdFeB@AC = 5.0 g/L, concentration of $Na_2S_2O_8$ = 300 mg/L, reaction time = 60 min), The coking wastewater chemical oxygen demand (COD) and total organic carbon (TOC) degradation ratio could reach 80.1% and 82.0%, respectively. In addition, a kinetics study indicated that the TOC of the coking wastewater degradation process follows a pseudo-first-order kinetics model. This novel catalyst has the advantage of producing no sludge during wastewater treatment, and the catalyst can be separated from the aqueous phase by the magnetic method. This innovative magnetic catalyst has good application prospects in solving organic industrial wastewater pollution.

Keywords: Coking wastewater; Persulfate; NdFeB; Magnetic activated carbon

1. Introduction

Coal is a key energy source in China for economic development [1]. With the development of the coal chemical industry, increases in coking wastewater cause serious threats to human health and the environment [2]. Coking wastewater is a kind of typical organic wastewater that has the characteristics of complex composition, high toxicity, and mutagenic and carcinogenic features [3]. Coking wastewater has gained increasing attention because it is difficult to degrade by common treatments such as biological, physical and chemical techniques [4–6]. Alternative technologies must be developed to solve this problem. Advanced oxidation processes (AOPs) have been extensively studied for the oxidation and destruction of hazardous organic pollutants [7–10]. Recently, AOPs based on activated persulfate (PS) have drawn attention in wastewater treatment and soil decontamination [11,12]. Organic pollutants could be degraded into innocuous and low-toxicity compounds or could be completely mineralized by an activated PS process treatment [13,14]. PS oxidation has been applied to degrade various contaminants such as polychlorinated biphenyls [15], gasoline or petroleum components [16], chlorophenols [17], and bisphenol A [18]. PS can be activated by heat and generated SO_4^-, which has strong oxidation characteristics, can react with most organic pollutants. Ag and Cu ions can also

* Corresponding author.

activate PS for pollutant degradation at normal temperatures and pressures. However, Ag and Cu ions can enter the aqueous phase during the oxidation process, which increases risks to environmental systems and human health. Therefore, an environment friendly catalyst such as Fe(II) [19] or activated carbon (AC) [20] has attracted attention. The reaction mechanisms of the PS oxidation process using ferrous ions as the catalyst are shown in reactions below (Eqs. (1)–(4)). Similar to the Fenton reactions, PS can be activated by Fe(II) to generate $\cdot SO_4^-$ and sulfate (Eq. (1)) [21]. The degradation rate can be enhanced through the activation of PS by Fe(II) to generate a reactive oxygen species (sulfate radicals, hydroxyl radicals and superoxide radical anions) (Eqs. (2)–(4)) [22]. In addition, Fe^{3+} can generate complexes with some aliphatic compounds, which react with persulfate to allow for the regeneration of Fe^{2+} [23].

$$Fe^{2+} + S_2O_8^{2-} \rightarrow Fe^{3+} + \cdot SO_4^- + SO_4^{2-} \quad (1)$$

$$\cdot SO_4^- + H_2O \rightarrow H^+ + SO_4^{2-} + \cdot OH \quad (2)$$

$$S_2O_8^{2-} + 2H_2O \rightarrow 2SO_4^{2-} + HO_2^- + 3H^+ \quad (3)$$

$$S_2O_8^{2-} + HO_2^- \rightarrow SO_4^{2-} + \cdot SO_4^- + \cdot O_2^- + H^+ \quad (4)$$

However, ferrous ion catalytic activity was significantly affected by the pH, and it also produced a large amount of sludge. Therefore, a heterogeneous catalyst, which has outstanding activity in acidic and alkaline conditions and produces little sludge, provides a promising alternative for the treatment of industrial wastewater [24,25]. Then, difficulty of separating catalysts from the treated water by a filtration process is a concern. Among numerous catalysts, magnetic solid catalysts are causing concern because they can be easily recycled by a magnetic separation method [26]. A magnetic catalyst such as magnetite (Fe_3O_4) has been studied and it also has good activity in catalysis [27]. It is well known that NdFeB is a kind of perfect magnetic material that has excellent magnetic characteristics [28]. AC, which has a large superficial area, can be employed as the catalyst substrate [29]. Therefore, the catalyst, which is a combination of NdFeB and AC, can be more efficient in the reaction. In this study, a novel magnetic catalyst with AC as a carrier has been synthesized. By spraying magnetic NdFeB powder onto the AC under negative pressure, magnetic NdFeB powder was loaded into the large holes of AC particles to form NdFeB magnetic AC (NdFeB@AC). Then, the FeO_x-NdFeB@AC catalyst was developed by loading Fe^{2+} on the NdFeB–AC through a negative pressure impregnation method. The magnetic properties, surface morphology and elementary composition of FeO_x-NdFeB@AC were tested. The effect of coking wastewater degraded by FeO_x-NdFeB@AC activated by a PS process was studied. The optimum conditions were investigated. The kinetics process of coking wastewater total organic carbon (TOC) degradation was also discussed.

2. Experimental procedure

2.1. Materials and reagents

Isotropy NdFeB powder (37–40 μm) was purchased from Nuode Limited Company (China). Walnut shell AC particles (0.3–2 mm), HNO_3 (65%), NaOH, H_2SO_4 (98%), and $Na_2S_2O_8$ were provided by Shenyang Chemical Reagent Limited Company (China). All chemicals were of analytical reagents grade and were used without further purification. Deionized water (18.2 MΩ cm, Smart-S15UVF, Hitech Instruments Co., Shanghai, China) was utilized in this work. The heterogeneous FeO_x-NdFeB@AC was fabricated using a negative pressure impregnation method as in a previous study [30]. Coking wastewater was collected from the wastewater treatment plant of a coal chemistry enterprise, located in Liaoning Province in China. Table 1 shows the main characteristics of coking wastewater used in this work.

Table 1
Basic characteristics of coking wastewater

pH	>9.0
COD (mg/L)	3,200–3,300
TOC (mg/L)	760–800
Dissolved oxygen (mg/L)	0
Electric conductivity (mS/cm)	2.104
Oxidation reduction potential (mV)	–439.9

2.2. Experimental procedures of degradation of coking wastewater

All batch experiments for coking wastewater degradation were performed in 500-mL beakers under mechanical stirring (100 rpm). A predetermined dosage of FeO_x-NdFeB@AC was dispersed in 300-mL solutions of coking wastewater, which were adjusted to the desired initial pH with 5% H_2SO_4 and 5% NaOH. Then, a certain amount of $Na_2S_2O_8$ solution was added, and the timing was started. Samples were taken every 5 min. Then, the TOC and chemical oxygen demand (COD) of the samples were measured immediately. Single-factor experiments were used to obtain the optimal parameters, such as the dosage of FeO_x-NdFeB@AC, $Na_2S_2O_8$ initial concentration, and pH. All experiments were carried out at least three times. The error of the results was less than 5%.

2.3. Characterization and analysis

An analysis of the catalyst surface and internal morphology was conducted by using field-emission scanning electron microscopy (SEM, XL-30, FEI, United States). Magnetite susceptibility measurements were performed at 300 K on a vibrating sample magnetometer (7407 Series, Lake shore, USA). X-ray diffraction (XRD) measurements were carried out on an XRD diffractometer (2500/PC, Rigaku, Japan). Fourier transform infrared spectrometer (FT-IR) analysis was carried out with an FT-IR (Cary630, Agilent, USA) in the range of 4,000–400 cm^{-1}. TOC was measured with a TOC analyzer (TOC-LCPH, Shimadzu, Japan). COD was measured with a COD analyzer (HI83099, Hanna, Italy). The COD and TOC degradation ratios were calculated by Eq. (5):

$$\eta(\%) = \frac{C_0 - C_t}{C_0} \times 100 \quad (5)$$

where η is the COD or TOC of the coking wastewater degradation ratio of reaction time t, C_0 is the initial COD or TOC

of the coking wastewater, and C_t is the COD or TOC of the coking wastewater in the reaction time.

3. Results and discussion

3.1. Characterization of FeO_x-NdFeB@AC

The magnetite characteristics of AC, NdFeB@AC, and FeO_x-NdFeB@AC were measured, and the results are presented in Fig. 1. The magnetic characteristics of AC were not obvious. However, FeO_x-NdFeB@AC has typical hard magnetic properties. The remanence and coercivity were 7.151 emu/g and 2,792.98 Oe, respectively. Even after sequencing the batch reaction five times (30 min of one sequencing reaction on the treatment coking wastewater under the optimal conditions that were obtained in this study), the FeO_x-NdFeB@AC had strong magnetism. The remanence and coercivity could reach 3.446 emu/g and 1,119.3 Oe, respectively, which means the catalyst could also be easily separated from water by the magnetic method. A surface morphology analysis of AC, NdFeB@AC, and FeO_x-NdFeB@AC was carried out by SEM, and the results are shown in Fig. 2. We can see from Fig. 2(a) that the surface of the AC had a porous structure. The surface of NdFeB@AC had a large number of NdFeB particles (Fig. 2(b)). However, most of these NdFeB particles adhered to the AC surface, and only a few NdFeB particles could move into the large pores of the AC. The adhesive force was large enough to ensure that a large number of NdFeB particles stayed in the original position, which can ensure the magnetic properties of the NdFeB@AC.

Fig. 2(c) shows that the FeO_x-NdFeB@AC surface morphology changes to a fluffy appearance. The picture shows that more NdFeB entered the large AC pores after negative pressure pretreatment, which indicates that the NdFeB could invade the large pores of AC with the $FeSO_4$ solution during the negative pressure impregnation process. Chemical components of the FeO_x-NdFeB@AC were analyzed using XRD. Fig. 3 shows the XRD patterns of FeO_x-NdFeB@AC. Peaks at 22.7° can be mainly indexed with active carbon. Extra peaks at 37.7°, 47.2°, and 53.6° were observed and can be indexed to the NdFeB. It was noted that the intensity of the NdFeB diffraction peak was prominent after the FeO_x-NdFeB@AC reaction. This is owing to iron ions on the surface of the catalyst that were consumed in reactions, and more NdFeB and AC was exposed. Therefore, more iron ions on the surface and more NdFeB into the AC big holes can increase the magnetism of the catalyst even after reactions, and it is also advantageous to the recycling of the catalyst.

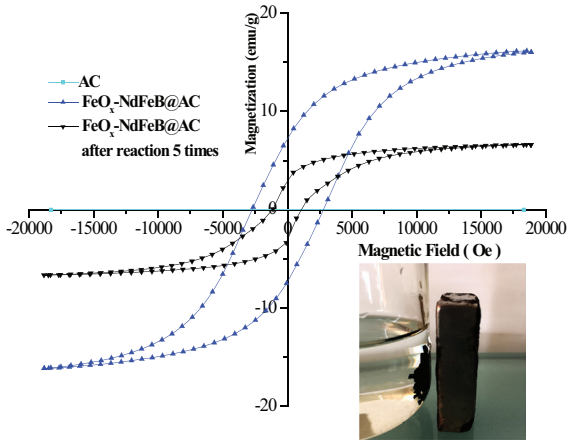

Fig. 1. Magnetization curve (at 300 K) of AC, FeO_x-NdFeB@AC, and FeO_x-NdFeB@AC after using five times. The inset shows a photograph of the FeO_x-NdFeB@AC (after five times reaction) attracted by a magnet.

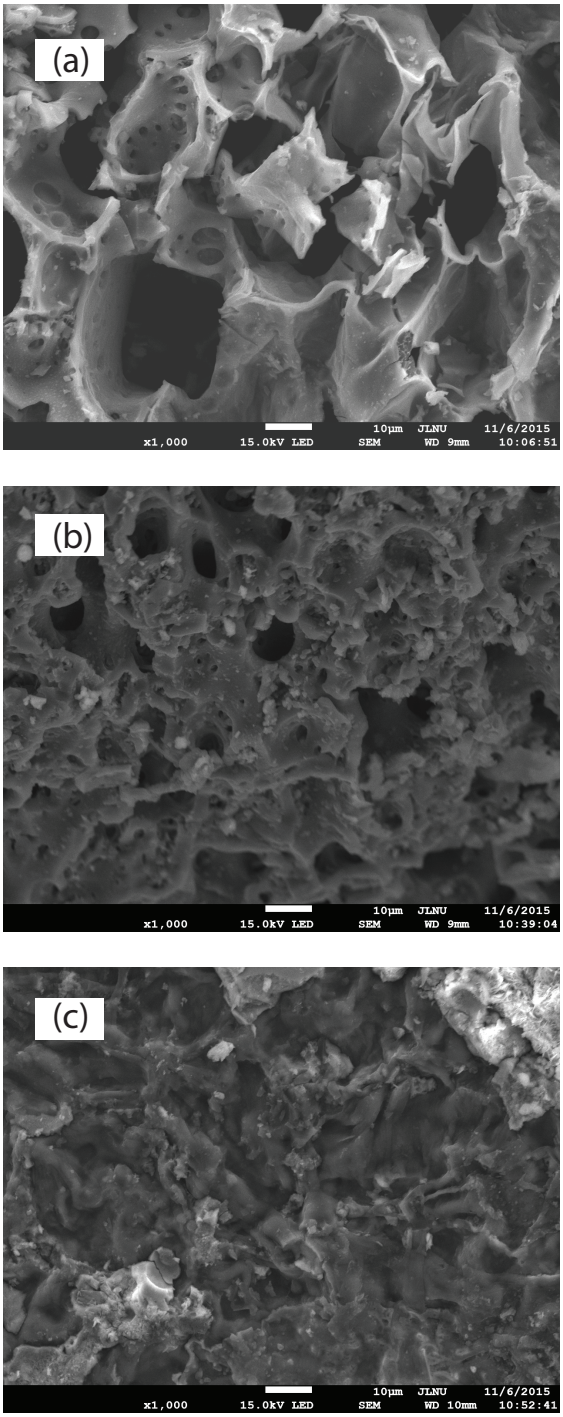

Fig. 2. SEM of FeO_x-NdFeB@AC. (a) AC surface (×1000); (b) NdFeB@AC surface (×1000); and (c) FeO_x-NdFeB@AC (×1000).

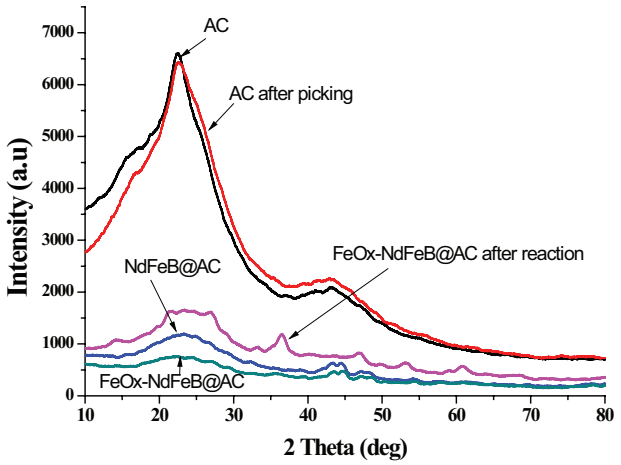

Fig. 3. XRD patterns of AC, AC after pickling, NdFeB@AC, FeO_x-NdFeB@AC, and FeO_x-NdFeB@AC after reaction.

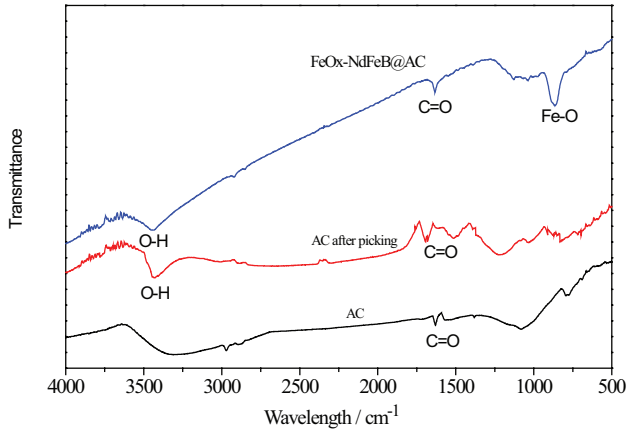

Fig. 4. FT-IR spectra of AC, AC after pickling, and FeO_x-NdFeB@AC.

The FT-IR spectra of AC, AC after pickling, and FeO_x-NdFeB@AC are presented in Fig. 4. IR bands appeared at approximately 3,400 cm^{-1} and were assigned to H–O bonds. All three samples had H–O bonds. However, the peak of the AC after pickling and the FeO_x-NdFeB@AC is more obvious than that of AC. It can be declared that after pickling, more –OH groups were obtained on the AC surface, which was beneficial to the next impregnation process. The frequency band at 1,632 cm^{-1} is attributed to the C=O bond, while the lower-frequency band at 865 cm^{-1} is ascribed to the vibration of the Fe–O bond in the samples.

3.2. Influence of initial pH value

The influence of the pH value on the degradation of coking wastewater in the reaction process with FeO_x-NdFeB@AC as a heterogeneous catalyst was investigated. The degradation reaction was maintained for 60 min under the conditions of 40°C temperature, 5.0-g/L catalyst dosages, and 300-mg/L initial concentrations of $Na_2S_2O_8$. The results are shown in Figs. 5(a) and 6(a). It can be seen that in the experimental range, the removal ratio of TOC and COD decreased rapidly with the increase in pH. The removal ratio of TOC dropped from 82.0% to 47.3% as the pH value increased from 3.0 to 9.0. The removal ratio of COD dropped from 80.1% to 68.5% when the pH value increased from 3.0 to 9.0. Therefore, a pH value of 3.0 was selected in the subsequent experimental study. This result is in accordance with that of Zhao et al. [31] and Zhang et al. [32]. In a word, a low pH value was helpful to the FeO_x-NdFeB@AC catalytic degradation of coking wastewater.

3.3. Influence of experimental temperature

The influence of temperature on the degradation of the coking wastewater process with FeO_x-NdFeB@AC catalyst was researched. The results are presented in Fig. 5(b). When the temperature was 20°C, 30°C, 40°C, 50°C, 60°C, and 70°C, the removal ratio of TOC was 54.6%, 67.9%, 82.0%, 81.8%, 82.6%, and 82.0%, respectively. The removal ratio of TOC could reach up to 82% when the temperature is 40°C. The removal ratio does not increase obviously when the temperature is higher than 40°C. Therefore, 40°C was selected as the optimal temperature for the subsequent experimental study. The COD removal ratio could reach 80.1% at the optimum temperature, which is illustrated in Fig. 6(b). The reaction temperature has great influence on the $Na_2S_2O_8$ decomposition to produce sulfate radicals (SO_4^-). The O–O bond will break more easily to produce SO_4^- in the high-temperature condition:

$$S_2O_8^{2-} + \text{Heat} \rightarrow 2{\cdot}SO_4^- \quad (6)$$

3.4. Influence of the initial concentration of the sodium persulfate

The influence of the $Na_2S_2O_8$ initial concentration on the degradation of coking wastewater was also investigated in this study. The initial concentration of $Na_2S_2O_8$ was changed, and other parameters were maintained at their optimum conditions. The experimental results are shown in Figs. 5(c) and 6(c). When the $Na_2S_2O_8$ initial concentration increased from 100 to 300 mg/L, the removal ratio of TOC increased from 41.5% to 82.0%. However, the removal ratio declined to 72.6% and 69.4% when the initial concentration of $Na_2S_2O_8$ reached 400 and 500 mg/L. The removal rate of COD also showed the same tendency. The removal ratio of COD increased to 80.1% when the $Na_2S_2O_8$ initial concentration was 300 mg/L. This might occur because a higher concentration of $Na_2S_2O_8$ leads to SO_4^- invalid consumption (such as in Eq. (3)). In this study, 300 mg/L of the $Na_2S_2O_8$ initial concentration was chosen as the optimum condition for subsequent research.

3.5. Influence of FeO_x-NdFeB@AC dosage

We considered the influence of the FeO_x-NdFeB@AC dosage on the degradation of coking wastewater under the conditions of temperature (40°C), pH value of 3.0, and 300 mg/L of $Na_2S_2O_8$. The results are presented in Figs. 5(d) and 6(d). Obviously, the FeO_x-NdFeB@AC dosage had a few effects on the removal rate of TOC when it increased to 5 g/L. When the FeO_x-NdFeB@AC dosage was 1.0, 3.0, 5.0, 10.0, and 15.0 g/L, the removal ratio of TOC was 61.2%, 70.7%, 82.0%, 69.3%,

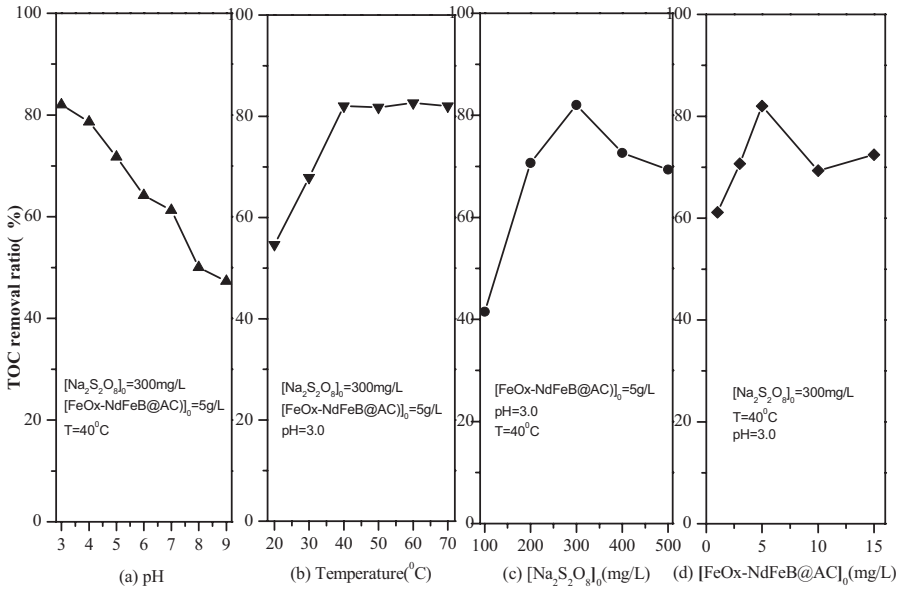

Fig. 5. Optimal conditions of coking wastewater TOC removal ratio by FeOx-NdFeB@AC activated persulfate process: (a) pH, (b) temperature, (c) $Na_2S_2O_8$ initial concentration, and (d) FeOx-NdFeB@AC initial concentration.

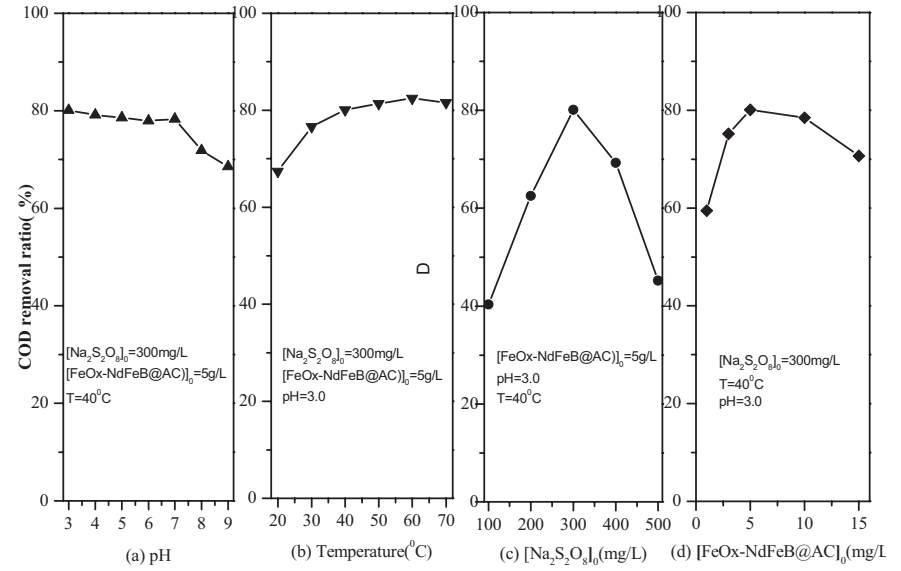

Fig. 6. Optimal conditions of coking wastewater COD removal ratio by FeOx-NdFeB@AC activated persulfate process. (a) pH, (b) temperature, (c) $Na_2S_2O_8$ initial concentration, and (d) FeOx-NdFeB@AC initial concentration.

and 72.4%, respectively, and the removal ratio of COD was 59.5%, 75.2%, 80.1%, 78.5%, and 70.7%, respectively. A catalyst dosing of 5.0 g/L was sufficient for pretreatment of this coking wastewater. When the catalyst dosage was above 5.0 g/L, it was not a sensitive parameter to control the reaction. Since the highest TOC and COD removal ratio could be above 80%, we selected 5.0 g/L FeO_x-NdFeB@AC in subsequent experiments.

3.6. Reaction kinetics studies on degradation of coking wastewater

The reaction kinetics in the experiment was discussed, and the results are presented in Table 2.The reaction kinetics was discussed in the experiment and the results are presented in Table 2. The TOC of coking wastewater degradation kinetics followed the pseudo-first-order kinetics model in different reaction periods. In the first 10 min, the reaction rate constant could reach 0.18 min^{-1}. The TOC of the wastewater declined rapidly, which could be attributed to the high concentration of $Na_2S_2O_8$ and more $\cdot SO_4^-$ generation at the beginning of the reaction. The reaction rate constant changed to 0.176 min^{-1} after 10 min of reaction. The intermediate products of coking wastewater degradation by PS could also be mineralized at a constant speed.

Table 2
Kinetic parameters of coking wastewater TOC degradation by heterogeneous PS

Pseudo-first order equation: $-\ln(C/C_0) = kt + a$			
	k (min^{-1})	R^2	a
0–10 min	0.180	0.949	0.128
10–60 min	0.176	0.918	–0.033

T = 40°C, $[FeO_x\text{-NdFeB@AC}]_0$ = 5 g/L, $[Na_2S_2O_8]_0$ = 300 mg/L, and reaction time = 60 min.

4. Conclusions

NdFeB magnetic AC was synthesized in this study. The FeO_x-NdFeB@AC was established by a method of negative pressure impregnation. The experimental results indicated that the catalyst had high catalytic activity. Under optimum conditions (T = 40°C, FeO_x-NdFeB@AC initial concentration of 5.0 g/L, $Na_2S_2O_8$ initial concentration of 300 mg/L, and pH 3.0), the TOC of the coking wastewater degradation rate could reach 82.0% after 60 min of reaction. The results of a kinetics study showed that the TOC degradation process followed pseudo-first-order kinetics. This catalyst could be easily separated and reused by the magnetic method. This catalyst has significant application prospects, and it also could provide a novel process for the degradation of organic pollutants.

Acknowledgment

This work was supported by the Key Program in Science and Technologies of Jilin Province (Grant No. 20150204049SF).

References

[1] Y. Liu, J. Liu, A. Zhang, Z. Liu, Treatment effects and genotoxicity relevance of the toxic organic pollutants in semi-coking wastewater by combined treatment process, Environ. Pollut., 220 (2017) 13–19.
[2] X. Yu, R. Xu, C. Wei, H. Wu, Removal of cyanide compounds from coking wastewater by ferrous sulfate: improvement of biodegradability, J. Hazard. Mater., 302 (2016) 468–474.
[3] F. Zhang, C. Wei, Y. Hu, H. Wu, Zinc ferrite catalysts for ozonation of aqueous organic contaminants: phenol and bio-treated coking wastewater, Sep. Purif. Technol., 156 (2015) 625–635.
[4] X. Ma, X. Wang, Y. Liu, J. Gao, Y. Wang, Variations in toxicity of semi-coking wastewater treatment processes and their toxicity prediction, Ecotoxicol. Environ. Safe., 138 (2017) 163–169.
[5] J.W. Shi, H. Deng, Z.P. Bai, S.F. Kong, X.Y. Wang, J.M. Hao, X.Y. Han, P. Ning, Emission and profile characteristic of volatile organic compounds emitted from coke production, iron smelt, heating station and power plant in Liaoning Province, China, Sci. Total Environ., 51 (2015) 101–108.
[6] X.P. Zhu, J.R. Ni, P. Lai, Advanced treatment of biologically pretreated coking wastewater by electrochemical oxidation using boron-doped diamond electrodes, Water Res., 43 (2009) 4347–4355.
[7] L. Zhu, Z. Ai, W. Ho, L. Zhang, Core–shell Fe–Fe_2O_3 nanostructures as effective persulfate activator for degradation of methyl orange, Sep. Purif. Technol., 108 (2013) 159–165.
[8] L.B. Chun, J.L. Wang, J. Dong, H.Y. Liu, X.L. Sun, Treatment of coking wastewater by an advanced Fenton oxidation process using iron powder and hydrogen peroxide, Chemosphere, 86 (2012) 409–414.
[9] M.J. Gao, W.D. Wang, M. Guo, M. Zhang, Contrast on COD photo-degradation in coking wastewater catalyzed by TiO_2 and TiO_2–TiO_2 nanorod arrays, Catal. Today, 174 (2011) 79–87.
[10] T. Zhang, L.L. Ding, H.Q. Ren, X. Xiong, Ammonium nitrogen removal from coking wastewater by chemical precipitation recycle technology, Water Res., 43 (2009) 5209–5215.
[11] L. Zhou, W. Zheng, Y. Ji, J. Zhang, C. Zeng, Y. Zhang, Ferrous-activated persulfate oxidation of arsenic(iii) and diuron in aquatic system, J. Hazard. Mater., 263 (2013) 422–430.
[12] Z. Dan, X. Liao, X. Yan, S.G. Huling, T. Chai, H. Tao, Effect and mechanism of persulfate activated by different methods for pahs removal in soil, J. Hazard. Mater., 254–255 (2013) 228–235.
[13] A.R. Ribeiro, O.C. Nunes, M.F.R. Pereira, A.M.T. Silva, An overview on the advanced oxidation processes applied for the treatment of water pollutants defined in the recently launched Directive 2013/39/EU, Environ. Int., 75 (2015) 33–51.
[14] F. Crapulli, D. Santoro, M.R. Sasges, A.K. Ray, Mechanistic modeling of vacuum UV advanced oxidation process in an annular photoreactor, Water Res., 64 (2014) 209–225.
[15] J. Zhao, Y. Zhang, X. Quan, S. Chen, Enhanced oxidation of 4-chlorophenol using sulfate radicals generated from zero-valent iron and peroxydisulfate at ambient temperature, Sep. Purif. Technol., 71 (2010) 302–307.
[16] S. Yang, X. Yang, X. Shao, R. Niu, L. Wang, Activated carbon catalyzed persulfate oxidation of azo dye acid orange 7 at ambient temperature, J. Hazard. Mater., 186 (2011) 659–666.
[17] C.H. Yen, Y.J. Chen, K.F. Chen, C.M. Kao, S.H. Liang, T.Y. Chen, Application of persulfate to remediate petroleum hydrocarbon-contaminated soil: feasibility and comparison with common oxidants, J. Hazard. Mater., 186 (2011) 2097–2102.
[18] C. Liang, K.J. Chang, Evaluation of persulfate oxidative wet scrubber for removing BTEX gases, J. Hazard. Mater., 164 (2009) 571–579.
[19] E. Kattel, M. Trapido, N. Dulova, Oxidative degradation of emerging micropollutant acesulfame in aqueous matrices by UVA-induced H_2O_2/Fe^{2+} and $S_2O_8^{2-}/Fe^{2+}$ processes, Chemosphere, 171 (2017) 528–536.
[20] X. Wang, L. Gu, P. Zhou, N. Zhu, C. Li, H. Tao, H. Wen, D. Zhang, Pyrolytic temperature dependent conversion of sewage sludge to carbon catalyst and their performance in persulfate degradation of 2-naphthol, Chem. Eng. J., 324 (2017) 203–215.
[21] H. Dong, Z. Qiang, J. Hu, C. Sans, Accelerated degradation of iopamidol in iron activated persulfate systems: roles of complexing agents, Chem. Eng. J., 316 (2017) 288–295.
[22] J. Yan, W. Gao, M. Dong, L. Han, L. Qian, C.P. Nathanail, M. Chen, Degradation of trichloroethylene by activated persulfate using a reduced graphene oxide supported magnetite nanoparticle, Chem. Eng. J., 295 (2016) 309–316.
[23] G. Fang, J. Gao, D.D. Dionysiou, C. Liu, D. Zhou, Activation of persulfate by quinones: free radical reactions and implication for the degradation of PCBs, Environ. Sci. Technol., 47 (2013) 4605–4611.
[24] H. Zhang, Z. Xiong, F. Ji, B. Lai, P. Yang, Pretreatment of shale gas drilling flowback fluid (SGDF) by the microscale Fe^0/persulfate/O_3 process (mFe^0/PS/O_3), Chemosphere, 176 (2017) 192–201.
[25] J. Yan, Y. Chen, L. Qian, W. Gao, D. Ouyang, M. Chen, Heterogeneously catalyzed persulfate with a CuMgFe layered double hydroxide for the degradation of ethylbenzene, J. Hazard. Mater., 338 (2017) 372–380.
[26] D. Xia, Y. Li, G. Huang, R. Yin, T. An, G. Li, H. Zhao, A. Lu, P.K. Wong, Activation of persulfates by natural magnetic pyrrhotite for water disinfection: efficiency, mechanisms, and stability, Water Res., 112 (2017) 236–247.
[27] P.K. Boruah, B. Sharma, I. Karbhal, M.V. Shelke, M.R. Das, Ammonia-modified graphene sheets decorated with magnetic Fe_3O_4 nanoparticles for the photocatalytic and photo-Fenton degradation of phenolic compounds under sunlight irradiation, J. Hazard. Mater., 325 (2017) 90–100.
[28] X.Y. Liu, Y.P. Li, L.X. Hu, Nanocrystalline NdFeB magnet prepared by mechanically activated disproportionation and desorption-recombination in-situ sintering, J. Magn. Magn. Mater., 330 (2013) 25–30.
[29] D. Xu, Y. Zhang, F. Cheng, P. Dai, Efficient removal of dye from an aqueous phase using activated carbon supported ferrihydrite as heterogeneous Fenton-like catalyst under assistance of

microwave irradiation, J. Taiwan Inst. Chem. Eng., 60 (2016) 376–382.
[30] C.W. Yang, D. Wang, Q. Tang, The synthesis of NdFeB magnetic activated carbon and its application in degradation of azo dye methyl orange by Fenton-like process, J. Taiwan Inst. Chem. Eng., 45 (2014) 2584–2589.
[31] Y.S. Zhao, C. Sun, J.Q. Sun, R. Zhou, Kinetic modeling and efficiency of sulfate radical-based oxidation to remove p-nitroaniline from wastewater by persulfate/Fe_3O_4 nanoparticles process, Sep. Purif. Technol., 142 (2015) 182–188.
[32] Y. Zhang, H.P. Tran, X. Du, I. Hussain, S. Huang, S. Zhou, W. Wen, Efficient pyrite activating persulfate process for degradation of p-chloroaniline in aqueous systems: a mechanistic study, Chem. Eng. J., 308 (2017) 1112–1119.